# Complex cells as cortically amplified simple cells

Frances S. Chance, Sacha B. Nelson and L.F. Abbott

*Volen Center and Department of Biology, Brandeis University, Waltham, Massachusetts 02454-9110, USA*
*Correspondence should be addressed to L.F.A. (abbott@volen.brandeis.edu)*

**The majority of synapses in primary visual cortex mediate excitation between nearby neurons, yet the role of local recurrent connections in visual processing remains unclear. We propose that these connections are responsible for the spatial-phase invariance of complex-cell responses. In a network model with selective cortical amplification, neurons exhibit simple-cell responses when recurrent connections are weak and complex-cell responses when they are strong, suggesting that simple and complex cells are the low- and high-gain limits of the same basic cortical circuit. Given the ubiquity of invariant responses in cognitive processing, the recurrent mechanism we propose for complex cells may be widely applicable.**



Although retinal input relayed through the lateral geniculate nucleus (LGN) of the thalamus clearly drives responses in the primary visual cortex (V1), LGN afferents account for only a small fraction of the synapses onto V1 neurons[1–7]. The primary source of synaptic input to neurons in primary visual cortex, at least in terms of numbers, is excitatory input from other nearby cortical neurons. What role do these local recurrent connections have in shaping the responses of V1 neurons to visual stimuli? One interesting idea is that recurrent connections amplify weak feedforward input signals from the LGN[8] and increase neuronal selectivity[8–11]. Neurons in the primary visual cortex are selective for a number of stimulus characteristics, including the orientation and direction of motion of light bars or gratings. Previous studies have suggested that cortical amplification may enhance orientation tuning[9–11] or direction selectivity[8]. Experiments in which cortical connections are disrupted by cooling or shocking the cortex suggest that recurrent connections do indeed amplify input signals, but they do not support the idea that this cortical amplification increases orientation or direction selectivity[12,13]. Thus, the functional role of recurrent connections in primary visual cortex remains unknown.

In previous models, cortical amplification has been used to increase neuronal selectivity[8–10]. Here we show that cortical amplification can also act to decrease selectivity. The effect on selectivity depends on the pattern of connectivity within the circuit. If neurons with similar selectivities excite each other, and those with different selectivities inhibit each other, selectivity is enhanced. If, on the other hand, neurons excite each other independently of their response tuning, selectivity is decreased. This is interesting with respect to the primary visual cortex where the responses of a class of neurons, the complex cells, exhibit little sensitivity to the spatial location of visual stimuli within their receptive fields.

Neurons in the primary visual cortex can be divided into two classes, simple and complex, based on the spatial separation or overlap of their responses to light and dark stimuli[14], and on their responses to bars[14] and sinusoidal gratings[15,16]. Here we focus on the responses to sinusoidal gratings. Simple cells are selective not only for the orientation of a grating, but also for its spatial frequency (the inverse of the distance over which the grating pattern repeats) and spatial phase (the position of the light and dark stripes of the grating within the receptive field). Complex cells, on the other hand, are selective for the orientation and spatial frequency of the grating, but not its spatial phase. Simple and complex cells can also be distinguished by the temporal modulation of their responses to drifting and counterphase gratings[15,16]. Simple-cell responses to a drifting grating are highly modulated, whereas complex-cell responses are relatively unmodulated. In response to a counterphase grating (a grating held stationary in space while its contrast oscillates sinusoidally in time; **Fig. 2**), simple-cell activity is modulated at the same frequency as the contrast of the stimulus. A complex-cell response varies at twice this frequency. These different temporal responses are a direct consequence of the lack of selectivity of the complex cell for spatial phase.

One way in which the spatial-phase-invariant responses of complex cells could arise is by pooling inputs with similar spatial-frequency and orientation preferences but different spatial-phase tunings. Previous models do this by having multiple feedforward inputs, from either simple cells[14] or sets of direct LGN afferents[17], converge onto a single complex cell. Another way of generating complex-cell responses is to square and sum the outputs of four simple cells with the same orientation and spatial-frequency tuning but spatial-phase preferences that are 90° apart[18,19]. One weakness of all these models is that they do not incorporate recurrent connections between complex cells, which seem to be particularly strong based on measurements of correlated firing[20]. We propose instead that an individual complex cell receives relatively weak feedforward inputs with a restricted range of spatial-phase preferences, and that spatial-phase invariance arises because of strong recurrent input from other complex cells.

In the recurrent model that we propose, complex cells are insensitive to spatial phase because of cortical amplification via recurrent connections. In other words, cortical amplification acts to reduce the phase selectivity of complex cells. Whereas previous models have used recurrent connections to increase selectivity of simple cells[8–11], we propose that recurrent connections are most relevant for complex cells, where they have the opposite

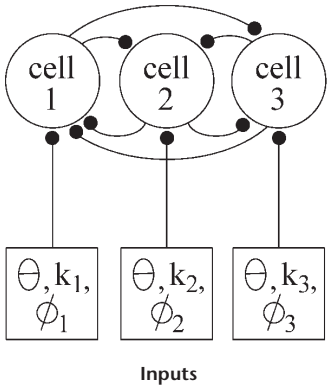


**Fig. 1.** The architecture of the recurrent model. The model neurons receive feedforward input that is selective for orientation, θ, spatial frequency, k, and spatial phase, ϕ. All inputs have the same orientation tuning and are given a realistic range of spatial-frequency and spatial-phase selectivities.

effect of reducing selectivity for spatial phase. This proposal is based on the suggestion that the efficacies of recurrent excitatory synaptic connections between pyramidal cells in primary visual cortex are independent of the spatial-phase preferences of the pre- and postsynaptic neurons. In a network model, we show that connections of this form generate simple-cell responses if the coupling is weak and complex-cell responses if it is strong.

## Results

We examined the effects of selective recurrent amplification by constructing a model network representing neurons in a single orientation column of primary visual cortex. All the neurons in the modeled column have the same orientation tuning. Each cell receives both feedforward and recurrent input (**Fig. 1**), and its response is described by a firing rate (see Methods). Without recurrent input, the model cells behave as simple cells because their feedforward input is computed from a simple-cell receptive field (see Methods). This corresponds to driving each model neuron with the output of a single simple cell. An important feature of the model is that the feedforward input is rectified, reflecting the fact that firing rates cannot be negative. This single nonlinearity is sufficient to generate nonlinear complex-cell responses in the model once recurrent connections are included.

Neurons in the network are labeled by the orientation, spatial-frequency and spatial-phase preferences of their inputs (**Fig. 1**). The strengths of the recurrent connections depend on the input-selectivity labels of the pre- and postsynaptic neurons. Because all the neurons in this model have the same orientation selectivity, the strength of the recurrent connections cannot vary with orientation preference. The scope of the model could easily be extended to a hypercolumn so that orientation-dependent synaptic strengths could be included. However, because this aspect of recurrent models has already been investigated[9,10], we focus on selectivity for spatial phase and spatial frequency.

The critical feature of the model we propose is that the strengths of the recurrent connections do not depend on the spatial-phase labels of the pre- and postsynaptic neurons. They do, however, depend on the spatial-frequency labels. We implement this by making the strength of the connection from a presynaptic neuron labeled by the preferred spatial frequency $k_{pre}$ to a postsynaptic neuron labeled by $k_{post}$ equal to a constant, $g$, multiplied by a function of $k_{pre} - k_{post}$. This function is chosen so that neurons with similar spatial-frequency preferences excite each other and those with different spatial-frequency preferences inhibit each other (see Methods). The overall strength of the recurrent coupling is determined by $g$. Stability of the model requires that $g$ be less than a maximum value $g_{max}$. A measure of the amplification due to the recurrent connections is the gain, given by $g_{max}/(g_{max} - g)$. When $g = 0$, the gain is unity, and as $g$ approaches $g_{max}$, the gain grows without bound. To keep the amplitude of the model responses roughly the same for different levels of gain, we reduce the strength of the feedforward input to each neuron when we increase the gain in the model. This allows us to concentrate on the effects of cortical amplification on response selectivity rather than on response amplitude.

The responses of one cell in the model network to a drifting grating are shown in Fig. 2a. When recurrent connections are absent, the response is highly modulated, like that of a simple cell. Increasing the gain of the network decreases the relative modulation of the response, and at a high level of gain there is almost no response modulation. Fig. 2b shows responses to a counterphase grating for various gains. At low gain, the model response oscillates at the same frequency as the stimulus, like the response of a simple cell. At moderate gain, the model exhibits a second, weaker response component in antiphase with the response at low gain. At high gain, the two response components are approximately equal in amplitude, and the response oscillates at twice the frequency of the stimulus, like that of a complex cell. Other neurons in the network respond similarly but have different spatial-phase and frequency selectivities (**Fig. 4**). Thus, the model neurons behave as simple cells at low gain and complex cells at high gain.

A measure commonly used to distinguish simple- and complex-cell responses to moving gratings is their relative modulation, which is calculated as the ratio of F1, the amplitude of response modulations at the same frequency as the stimulus, to F0, the unmodulated component of the response. Cells are considered complex if F1/F0 is less than one[21]. We examined how this ratio varies as a function of $g/g_{max}$ (**Fig. 3**). The relationship is linear, because the spatial-phase-invariant F0 component is amplified by the gain factor $g_{max}/(g_{max} - g)$ while the spatial-phase-specific F1 component is unamplified. As a result, F1/F0 is proportional to $1 - g/g_{max}$. The model responses are complex if $g/g_{max}$ is greater

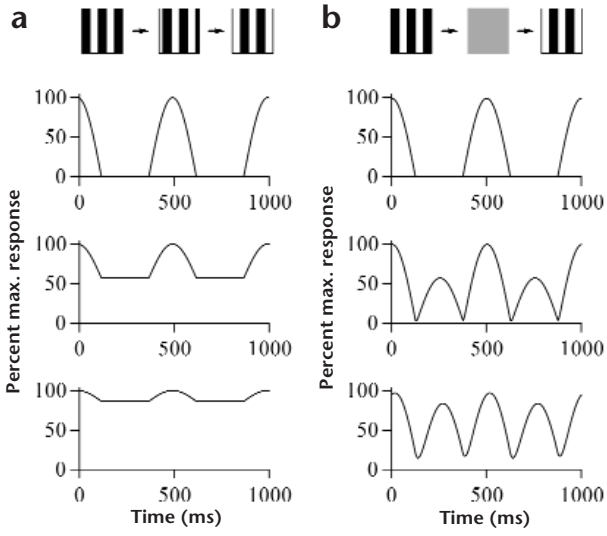


**Fig. 2.** The effects of recurrent input on model responses. Schematics of drifting and counterphase gratings are shown at the top. (The schematics are not aligned with the graphs.) In both (a) and (b), the level of gain from top to bottom graphs is one, five and twenty. **(a)** The response of a model cell to a 2-Hz drifting grating for different network gains. **(b)** Responses of the same cell to a 2-Hz counterphase grating for different gains.

than 0.36 and simple if $g/g_{max}$ is less than this value.

Figure 4a shows the spatial-phase tuning of three different neurons that exhibit complex-cell responses, selected from a network of 256 cells at high gain. Reduction of spatial-phase dependence does not imply that all selectivity is absent. For example, the cells show spatial-frequency tuning (**Fig. 4b**). The preferred spatial frequency of a given cell in the network is determined by both the selectivity of its feedforward input and its recurrent couplings. The width of its spatial-frequency tuning curve is primarily determined by the recurrent connections. Ranges of preferred values for other characteristics such as orientation selectivity can arise in a similar manner from appropriately tuned recurrent connections (not shown). Thus cortical amplification can increase selectivity for some attributes (such as spatial frequency) while decreasing it for others (such as spatial phase) within the same circuit.

In the networks discussed thus far, all cells operated at the same gain, and thus all were simple at low gain and complex at high gain. It is possible to construct a network in which some cells operate at low gain and others at high gain by varying the strength of the recurrent input from cell to cell (see Methods). The result is a network with a mixture of simple and complex cells (**Fig. 5**). Note that the different simple cells in this network have different spatial-phase preferences.

Finally we examine how the responses of the model depend on temporal frequency, and compare frequency–response curves for drifting and counterphase gratings. As previously noted[21], temporal-frequency tuning curves for complex cells responding to drifting gratings can be significantly broader than those measured in response to counterphase gratings (**Fig. 6a**). This result is interesting with regard to models of complex cells, because it provides a possible means of distinguishing between feedforward and recurrent models.

In the recurrent model, most of the input to a complex cell arises from other complex cells. For a drifting grating, this complex-cell input is unmodulated, and for a counterphase grating, it varies at twice the frequency of the stimulus (**Fig. 2**). Thus, the frequency of the input to a complex cell in the recurrent model is different for these two stimuli. Drifting and counterphase gratings can then give rise to different temporal-frequency tuning curves if the integration of synaptic inputs in the complex cell is frequency dependent. One way to incorporate such a mechanism is to introduce short-term depression at the synapses of the model.

We have recently studied how the temporal-response properties of simple cells are affected by synaptic depression[22], which has been measured at intracortical synapses in slices of primary visual cortex[23]. To test whether synaptic depression could have a similar role in complex-cell responses, we included it at the synapses of the model (see Methods). In many ways, synaptic depression of recurrent synapses has a similar effect on model complex-cell responses as it did on simple-cell responses in our previous work[22], enhancing transients and increasing the bandpass character of the response. In addition, synaptic depression causes the temporal-frequency tuning curve for drifting gratings to be broader than for counterphase gratings (**Fig. 6b**), as has been observed previously[21]. For the case of a drifting grating, as mentioned above, the input to a complex cell in the model arises primarily from other complex cells firing at constant rates. The broadening of the response for a drifting grating occurs because synaptic depression decreases the sensitivity of the postsynaptic cell to the magnitudes of presynaptic mean firing rates[24,25]. When the stimulus is a counterphase grating, the input firing rates oscillate. In this case, the bandpass properties of synaptic depression sharpen the temporal-

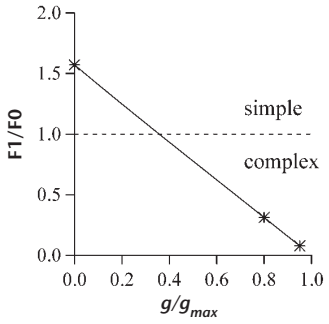


**Fig. 3.** The relative modulation of the response of the model cells to a drifting 2-Hz grating as a function of $g/g_{max}$, the strength of the recurrent connections relative to the maximum stable strength. The three cases shown in Fig. 2 are indicated by asterisks.

frequency tuning curve[22]. The key feature of the recurrent model that allows these curves to be different is that the complex-cell input is different for drifting and counterphase gratings.

In the classic feedforward model of Hubel and Wiesel[14], complex-cell responses are the result of convergent input from a population of simple cells. Simple cells respond similarly to drifting and counterphase gratings (**Fig. 2**). The frequencies of the inputs to a complex cell are therefore identical, in the feedforward model, for these two types of stimuli. Complex cells in the feedforward model respond differently to counterphase and drifting gratings because the relative temporal phases, not the frequencies, of their inputs are different (for a counterphase grating, the inputs are synchronous, whereas for a drifting grating they are asynchronous). Because the frequencies of the inputs are identical in the two cases, complex-cell temporal-frequency tuning curves in response to drifting and counterphase gratings are predicted to be the same (**Fig. 6c**). For comparison, we have included synaptic depression at the synapses of the feedforward model (see Methods), which makes the transient and bandpass charac-

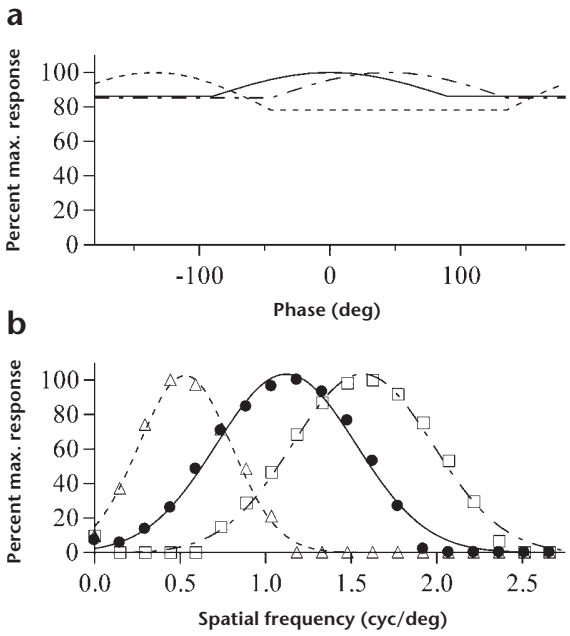


**Fig. 4.** At high gain, the model cells are not selective for spatial phase but retain different selectivities for spatial frequency. **(a)** The spatial-phase tuning curves of three representative neurons in a model network of 256 cells at a gain of twenty. **(b)** The spatial-frequency tuning curves of the same three neurons in the network.

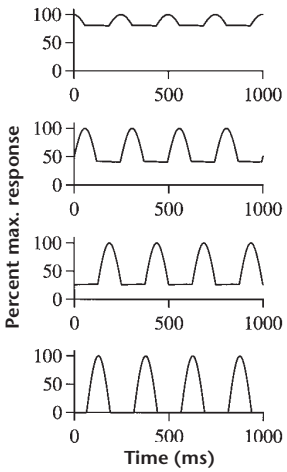


**Fig. 5.** Four representative neurons from a model network with a mixture of simple and complex cells. The responses shown are to a 4-Hz drifting grating. The upper two panels show two model neurons with complex responses. The neuron in the second panel has a higher F1/F0 ratio than the neuron in the top panel, but both are less than one. The two lower panels show simple cells with different spatial-phase preferences.

ter of its responses similar to those of the recurrent model.

The frequency dependence of synaptic depression causes the degree of 'complexness' of the neuronal responses in the recurrent model to vary as a function of temporal frequency. Furthermore, this variation is different for drifting and counterphase gratings (**Fig. 7**). The lower trace shows the relative modulation of a complex-cell response (F1/F0) as a function of the temporal frequency of a drifting grating. By this measure, the response becomes more complex (smaller F1/F0) at the lower and higher ranges of drift frequency. Another related measure is the ratio of F1 to F2 in response to a counterphase grating, as shown in the upper trace of **Fig. 7**. By this measure, the model shows an opposite trend. The F1/F2 ratio increases at higher and lower frequencies, indicating that, for counterphase gratings, the model behavior becomes more like that of a simple cell in these frequency ranges. It should be straightforward to test these predictions experimentally. In the feedforward model, we found that F1/F0 and F1/F2 are independent of temporal frequency.

## Discussion

In both the Hubel and Wiesel model[14] and our recurrent model, the feedforward inputs to complex cells arise from simple cells. A recent study[26] provided evidence for monosynaptic excitatory connections from simple to complex cells. However, complex cells can also receive input directly from the LGN[27–29], and it is possible to excite complex cells without strong excitation of simple cells[30–35]. Although our recurrent model requires only weak feedforward input, the simple-cell input we used could be replaced by LGN input if this were integrated in an appropriate nonlinear manner. One feedforward model[17] used voltage-dependent dendritic conductances to achieve nonlinear integration. A similar approach could probably be used in the recurrent model.

To keep the model as simple as possible, we used purely excitatory feedforward input. The presence of feedforward inhibition would tend to make the neurons appear less complex, because the magnitude of the unmodulated response to a drifting grating would be reduced. This shifts the F1/F0 curve (**Fig. 3**) to the right, which would probably make it more realistic. Simple cells have been estimated to operate at a gain of about two or three[12]. According to Fig. 3, this would put these cells into the complex range, but with inhibition a model cell can remain simple even at this high a gain.

We have followed standard neural-network modeling practice and used a first-order differential equation to describe the firing rates of neurons in the network (see Methods). This, of course, provides only a crude approximation of real neuronal dynamics. The temporal dynamics of the model are not important for producing the phase-invariant complex-cell responses. However, the frequency–response curves of Figs. 6 and 7 could change if the basic differential equation of the model were modified significantly.

In the proposed model, complex-cell responses arise through recurrent amplification of simple-cell responses. Simple and complex cells represent the weakly and highly coupled regimes of the same basic cortical circuit. In the Results, we suggest ways of testing this hypothesis and distinguishing the recurrent model from feedforward models, based on comparing the amplitude and various measures of 'complexness' for responses to drifting and counterphase gratings of different frequencies. A more direct, though more difficult, way of testing the model is to manipulate the strengths of recurrent cortical connections by pharmacological techniques, cooling or shocking. The model predicts that any manipulation that weakens the effects of intracortical excitation will make complex cells act more like simple cells. Conversely, manipulations that increase the effectiveness of recurrent excitation should make simple cells respond more like complex cells. Some results along these lines have been reported. Blocking inhibition, which may increase the cortical gain by enhancing the effect of recurrent excitation, seems to make simple cells behave more like complex cells[36] (see also D.E. Shulz *et al.*, *Soc. Neurosci. Abstr.* **19**, 628, 1993). Others have also proposed a model in which simple- and complex-cell responses are formed by the same cortical circuit[37,38]. In that model, however, inhibition makes com-

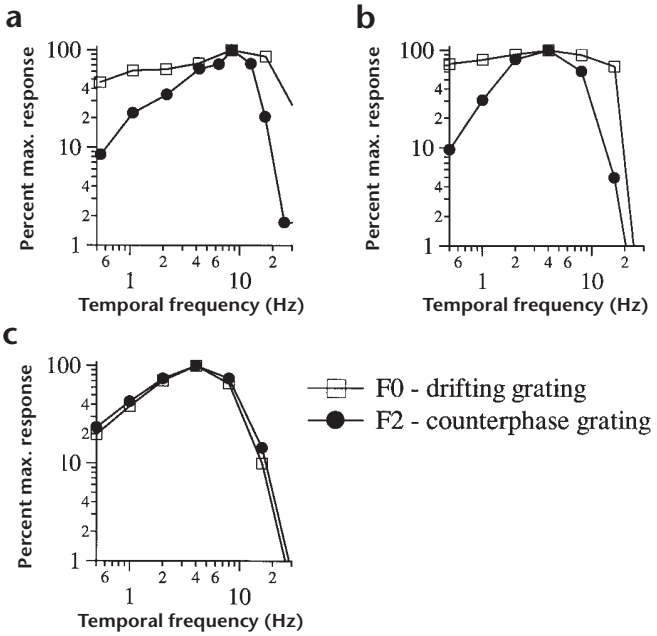


**Fig. 6.** Temporal-frequency tuning curves of F2 (the amplitude of the response at twice the stimulus frequency) and F0 (the amplitude of the unmodulated response) components in response to counterphase and drifting gratings. **(a)** Replotted data from ref. 21. The F2 temporal-frequency tuning curve of a complex-cell response to a counterphase grating is narrower than the F0 tuning curve in response to a drifting grating. **(b)** In the recurrent model with synaptic depression, the temporal-frequency tuning curve in response to a counterphase grating is also narrower than the tuning curve in response to a drifting grating. **(c)** In the Hubel and Wiesel feedforward model[14] with synaptic depression, the tuning curves are not significantly different.

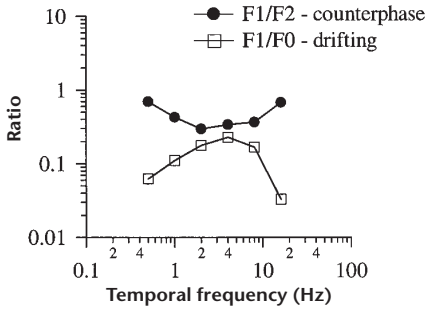


**Fig. 7.** Measures of complexity vary as a function of temporal frequency. Upper curve, the ratio F1/F2 for a model complex cell in response to counterphase gratings. Lower curve, the relative modulation F1/F0 of model complex-cell responses to drifting gratings. For both of these measures, smaller values correspond to more complex responses.

plex cells simple, whereas in our model recurrent excitation makes simple cells complex.

Amplification by recurrent cortical circuitry can either increase or decrease selectivity. Although most attention has focused on increasing selectivity by this mechanism, decreases of selectivity could also be important in cortical processing. Cortical amplification through recurrent connections, used here to produce complex-cell responses that are spatial-phase invariant, may be a general mechanism for generating invariant representations of input data.

## Methods

Each neuron in the network model receives feedforward and recurrent input. The activity of neuron $i$, described by a firing rate $r_i$, is determined by the sum of the two inputs through the standard rate-model equation

$$\tau_r \frac{dr_i}{dt} = I_i^{ff} + I_i^{rec} - r_i$$

where $I_i^{ff}$ and $I_i^{rec}$ represent the feedforward and recurrent inputs. Studies suggest that under conditions in which a neuron receives many inputs, the time constant in this equation, $\tau_r$, is small, close to the synaptic time constant and not equal to the membrane time constant[9,39]. Therefore, we have chosen $\tau_r = 1$ ms.

The feedforward input is equal to the response of a simple cell with a Gabor receptive field and a standard temporal-response function. We restrict the stimuli to those of optimal orientation; therefore we write the stimulus as a function of a single spatial variable. For a stimulus with contrast $s(x,t)$, the feedforward input is

$$I_i^{ff} = A\left[\int dx G_i(x) \int_0^\infty dt' H(t') s(x, t-t')\right]_+$$

where the notation $[\ ]_+$ stands for rectification. The parameter $A$ is adjusted so that the amplitude of the neuron's response remains relatively constant for different levels of gain. The spatial filter is a Gabor function,

$$G_i(x) = e^{-\frac{x^2}{2\sigma_i^2}} \cos(k_i x - \phi_i)$$

where $\sigma_i$ determines the spatial extent of the receptive field, $k_i$ is the preferred spatial frequency, and $\phi_i$ is the preferred spatial phase. $\sigma_i$ is chosen such that $k_i \sigma_i = 2.5$, which gives the neurons a realistic bandwidth. In the model presented here, the values of $\phi_i$ are equally distributed over the interval $[-180^\circ, 180^\circ]$. The value of $k_i$ ranges from 0 to 3.5 cycles/degree. The temporal response function is[18]

$$H(t') = e^{-\alpha t'}\left(\frac{(\alpha t')^5}{5!} - \frac{(\alpha t')^7}{7!}\right)$$

and we use $\alpha = 1$/ms.

A counterphase grating is created by sinusoidally modulating the contrast at a temporal frequency $\omega$, $s(x,t) = \cos(Kx - \Phi)\cos(\omega t)$, where $K$ is the spatial frequency of the grating and $\Phi$ is its spatial phase. In all figures except Fig. 4b, the optimal value of $K$ for the neuron in the figure is used. For a drifting grating, the contrast is held constant but the spatial phase of the grating is a function of time, $s(x,t) = \cos(Kx - \omega t)$ where $\omega/K$ is the drift velocity.

The recurrent input to model cell $i$ is given by

$$I_i^{rec} = \frac{g_i}{(N-1)} \sum_{j \neq i}^{N} \left(2e^{-\frac{(k_i - k_j)^2}{2\sigma_c^2}} - e^{-\frac{(k_i - k_j)^2}{2\sigma_s^2}}\right) r_j$$

where $0 \le g_i < g_{max}$, N is the number of cells in the network, $r_j$ is the activity of neuron $j$, and $k_i$ and $k_j$ represent the spatial-frequency selectivities of the feedforward inputs to neurons $i$ and $j$. The spatial-frequency tuning curve width is primarily determined by $\sigma_c = 0.5$ cycles/deg and $\sigma_s = 1$ cycle/deg. In all but Fig. 5, all the values of $g_i$ are the same. In Fig. 5, the $g_i$ values were chosen randomly over the allowed range.

We incorporate synaptic depression using a previously developed model[23,24]. The feedforward input transmitted to cell $i$ is now $D_i^{ff} I_i^{ff}$, where $I_i^{ff}$ is calculated as described above, and $0 \le D_i^{ff} \le 1$ represents the level of depression for the feedforward input synapse to neuron $i$. $D_i^{ff}$ is determined by[23,24]

$$\tau_D \frac{dD_i^{ff}}{dt} = 1 - D_i^{ff}\left(1 + \tau_D I_i^{ff}(1-d)\right)$$

where $d$ and $\tau_D$ control the rate of depression onset and the time constant of recovery from depression. We took $d = 0.95$ and $\tau_D = 300$ ms. When depression is included, the recurrent input to neuron $i$ is modified so that

$$I_i^{rec} = \frac{g_i}{(N-1)} \sum_{j \neq i}^{N} D_{ij}^{rec}\left(2e^{-\frac{(k_i - k_j)^2}{2\sigma_c^2}} - e^{-\frac{(k_i - k_j)^2}{2\sigma_s^2}}\right) r_j$$

where $0 \le D_{ij} \le 1$ represents the level of depression for the synapse from neuron j to neuron i. It is determined by

$$\tau_D \frac{dD_{ij}^{rec}}{dt} = 1 - D_{ij}^{rec}\left(1 + \tau_D r_j (1-d)\right)$$

When depression was included, synaptic transmission only occurred for presynaptic firing rates above 0.5 Hz to stabilize the network.

In the Hubel and Wiesel feedforward model[14], a complex cell arises from $M$ converging simple-cell inputs with a range of spatial-phase preferences. When synaptic depression is added to the model, the activity of cell $i$ is determined by the sum of its feedforward inputs

$$\tau_r \frac{dr}{dt} = \sum_i^M D_i^{ff} I_i^{ff} - r$$

where $I_i^{ff}$ and $D_i^{ff}$ are calculated as described above.

## Acknowledgements

*Research supported by the Sloan Center for Theoretical Neurobiology at Brandeis University, the National Science Foundation (DMS-95-03261), the W.M. Keck Foundation, the National Eye Institute (EY-11116) and the Alfred P. Sloan Foundation.*

RECEIVED1 DECEMBER 1998; ACCEPTED 26 JANUARY 1999

1. McGuire, B. A., Hornung, J. P., Gilbert, C. D. & Wiesel, T. N. Patterns of synaptic input to layer 4 of cat striate cortex. *J. Neurosci.* **4,** 3021–3033 (1984).
2. Kisvarday, Z. F. *et al.* Synaptic targets of HRP-filled layer III pyramidal cells in the cat striate cortex. *Exp. Brain Res.* **64,** 541–542 (1986).
3. LeVay, S. Synaptic organization of claustral and geniculate afferents to the visual cortex of the cat. *J. Neurosci.* **6,** 3564–3575 (1986).
4. White, E. L. *Cortical Circuits: Synaptic Organization of the Cerebral Cortex* (Birkauser, Boston, 1989).
5. Braitenberg, V. & Schüz, A. *Anatomy of the Cortex* (Springer, Berlin, 1991).
6. Peters, A. & Payne, B. R. Numerical relationships between geniculocortical afferents and pyramidal cell modules in cat primary visual cortex. *Cereb. Cortex* **3,** 69–78 (1993).
7. Peters, A. & Payne, B. R. A numerical analysis of the geniculocortical input to striate cortex in the monkey. *Cereb. Cortex* **4,** 215–229 (1994).

8. Douglas, R. J., Koch, C., Mahowald, M., Martin, K. A. C. & Suarez, H. H. Recurrent excitation in neocortical circuits. *Science* **269,** 981–985 (1995).
9. Ben-Yishai, R., Bar-Or, L. & Sompolinsky, H. Theory of orientation tuning in visual cortex. *Proc. Natl. Acad. Sci. USA* **92**, 3844–3848 (1995).
10. Somers, D. C., Nelson, S. B. & Sur, M. An emergent model of orientation selectivity in cat visual cortical simple cells. *J. Neurosci.* **15**, 5448–5465 (1995).
11. Sompolinsky, H. & Shapley, R. New perspectives on the mechanisms for orientation selectivity. *Curr. Opin. Neurobiol.* **7,** 514–522 (1997).
12. Ferster, D., Chung, S. & Wheat, H. Orientation selectivity of thalamic input to simple cells of cat visual cortex. *Nature* **380,** 249–252 (1996).
13. Chung, S. & Ferster, D. Strength and orientation tuning of the thalamic input to simple cells revealed by electrically evoked cortical suppression. *Neuron* **20,** 1177–1189 (1998).
14. Hubel, D. H. & Wiesel, T. N. Receptive fields, binocular interaction and functional architecture in the cat's visual cortex. *J. Physiol. (Lond.)* **160,** 106–154 (1962).
15. Movshon, J., Thompson, I. & Tolhurst, D. Spatial summation in the receptive fields of simple cells in the cat's striate cortex. *J. Physiol. (Lond.)* **283,** 53–77 (1978).
16. Movshon, J., Thompson, I. & Tolhurst, D. Receptive field organization of complex cells in cat's striate cortex. *J. Physiol. (Lond.)* **283,** 79–99 (1978).
17. Mel, B. W., Ruderman, D. L. & Archie, K. A. Translation–invariant orientation tuning in visual complex cells could derive from intradendritic computations. *J. Neurosci.* **18,** 4325–4334 (1998).
18. Adelson, E. H. & Bergen, J. R. Spatiotemporal energy models for the perception of motion. *J. Opt. Soc. Am. A* **2,** 284–299 (1985).
19. Pollen, D. A. & Ronner, S. F. Phase relationships between adjacent simple cells in the visual cortex. *Science* **212,** 1409–1411 (1981).
20. Toyama, K., Kimura, M. & Tanaka, K. Organization of cat visual cortex as investigated by cross–correlation technique. *J. Neurophysiol.* **46,** 202–214 (1981).
21. Hawken, M. J., Shapley, R. M. & Grosof, D. H. Temporal-frequency selectivity in monkey visual cortex. *Vis. Neurosci.* **13,** 477–492 (1996).
22. Chance, F. S., Nelson, S. B. & Abbott, L. F. Synaptic depression and the temporal response characteristics of V1 cells. *J. Neurosci.* **18,** 4785–4799 (1998).
23. Varela, J. A. *et al.* A quantitative description of short-term plasticity at excitatory synapses in layer 2/3 of rat primary visual cortex. *J. Neurosci.* **17,** 7926–7940 (1997).
24. Abbott, L. F., Varela, J. A., Sen, K. & Nelson, S. B. Synaptic depression and cortical gain control. *Science* **275,** 220–224 (1997).
25. Tsodyks, M. V. & Markram, H. The neural code between neocortical pyramidal neurons depends on neurotransmitter release probability. *Proc. Natl. Acad. Sci. USA* **94,** 719–723 (1997).
26. Alonso, J.-M. & Martinez, L. M. Functional connectivity between simple cells and complex cells in cat striate cortex. *Nat. Neurosci.* **1,** 395–403 (1998).
27. Hoffman, K. P. & Stone, J. Conduction velocity of afferents of cat visual cortex: a correlation with cortical receptive field properties. *Brain Res.* **32,** 460–466 (1971).
28. Singer, W., Tretter, F. & Cynader, M. Organization of cat striate cortex: a correlation of receptive-field properties with afferent and efferent connections. *J. Neurophysiol.* **38,** 1080–1098 (1975).
29. Ferster, D. & Lindström, S. An intracellular analysis of geniculo-cortical connectivity in area 17 of the cat. *J. Physiol. (Lond.)* **342,** 181–215 (1983).
30. Hammond, P. & MacKay, D. M. Differential responses of cat visual cortical cells to textured stimuli. *Exp. Brain Res.* **22,** 427–430 (1975).
31. Movshon, J. A. The velocity tuning of single units in cat striate cortex. *J. Physiol. (Lond.)* **249,** 445–468 (1975).
32. Hammond, P. & MacKay, D. M. Differential responsiveness of simple and complex cells in cat striate cortex to visual texture. *Exp. Brain Res.* **30,** 275–296 (1977).
33. Malpeli, J. G. Activity of cells in area 17 of the cat in absence of input from layer A of lateral geniculate nucleus. *J. Neurophysiol.* **49,** 595–610 (1983).
34. Malpeli, J. G., Lee, C., Schwark, H. D. & Weyand, T. G. Cat area 17. I. Pattern of thalamic control of cortical layers. *J. Neurophysiol.* **56,** 1062–1073 (1986).
35. Mignard, M. & Malpeli, J. G. Paths of information flow through visual cortex. *Science* **251,** 1249–1251 (1991).
36. Sillito, A. M. The contribution of inhibitory mechanisms to the receptive field properties of neurones in the striate cortex of the cat. *J. Physiol. (Lond.)* **250,** 305–329 (1975).
37. Borg-Graham, L. J., Monier, C. & Frégnac, Y. Visual input evokes transient and strong shunting inhibition in visual cortical neurons. *Nature* **393,** 369–373 (1998).
38. Debanne, D., Shulz, D. E. & Frégnac, Y. Activity-dependent regulation of 'on' and 'off' responses in cat visual cortical receptive fields. *J. Physiol. (Lond.)* **508,** 523–548 (1998).
39. Treves, A. Mean-field analysis of neuronal spike dynamics. *Network* **4,** 259–284 (1993).